Nanocrystallization behaviour and optimized magnetoimpedance effect in FeZrBNbCu alloys

2007 J. Phys. D: Appl. Phys. 40 6507

(http://iopscience.iop.org/0022-3727/40/21/006)

IOP Publishing Journal of Physics D: Applied Physics
J. Phys. D: Appl. Phys. **40** (2007) 6507–6513 doi:10.1088/0022-3727/40/21/006

Nanocrystallization behaviour and optimized magnetoimpedance effect in FeZrBNbCu alloys

Ke Zhang[1], Bing Han[1,4], Li Xiao[2], Zhong Hua[2], Dawei Zhou[1], Tao Zhang[1], Xiaobo Du[1], Bin Yao[1,3,5], Xianchao Xun[1] and De Wang[1]

[1] Department of Physics, Jilin University, 2519 Jiefang Road, Changchun 130023, People's Republic of China
[2] Department of Physics, Jilin Normal University, Siping 136000, People's Republic of China
[3] Key Laboratory of Excited State Process, Changchun Institute of Optics, Fine Mechanics and Physics, Chinese Academy of Sciences, Changchun 130022, People's Republic of China
[4] College of Zhuhai, Jilin University, Zhuhai 519041, People's Republic of China

E-mail: binyao@mail.jlu.edu.cn

Received 5 March 2007, in final form 2 September 2007
Published 19 October 2007
Online at stacks.iop.org/JPhysD/40/6507

Abstract
The work aims at understanding the changes in magnetic properties and the magnetoimpedance (MI) effect for the $Fe_{84.5}Zr_4B_{8.5}Nb_2Cu_1$ (FZBNC) nanocrystalline alloys with the annealing temperature (T_a) from the microstructure point of view. The as-quenched FZBNC ribbons were annealed in a vacuum condition at selected temperatures for 20 min. The microstructures of the specimens were examined by the x-ray diffraction technique. The bcc α-Fe phase is identified from the XRD patterns. The mean grain size of the α-Fe phase (D_1) at different annealing temperatures (T_a) was estimated using Scherrer's equation. The results show that D_1 for the sample annealed at 575 °C is about 20 nm, which is the smallest value among all the samples. Measurements on the MI effect reveal that the FZBNC ribbon annealed at 575 °C exhibits the most drastic MI ratio of 756% at 600 kHz accompanied by the field sensitivity of 108% Oe^{-1}, while a large MI effect is not observed in the sample annealed at other temperatures. The origin of the excellent MI effect is investigated in this paper.

1. Introduction

Nanocrystalline magnets have attracted attention from all over the world for use as power transformers, inductors, data communication interface components and high moment underlayers for perpendicular recording media, etc [1–3]. In particular, nanostructured materials with good soft magnetic properties have been investigated for suitable use as magnetic heads and sensors based on the magnetoimpedance (MI) effect, which consists of a change in the total impedance of a magnetic conductor under the application of a magnetic field. Since its discovery [4, 5], the MI effect has been intensively studied due to the fact that it can be not only applied in the magnetic field sensors but also used as a powerful tool in the study of magnetization in a wide range of frequencies. The field and stress dependence of MI also helps in studying some basic magnetic properties such as the anisotropy field (H_k) and magnetostriction coefficient (λ_s) [6]. Up to now, the MI effect has been investigated in a variety of Co- and Fe-based wires, ribbons, thin films, multilayers, etc. [7–16].

Many research results have confirmed that the MI effect is closely associated not only with soft magnetic properties but also with magnetic anisotropy. Magnetic anisotropy in some amorphous alloys is dominated by magnetostrictive phenomena. The alloy composition determines the value of the magnetostrictive constant, whereas the fabrication process and annealing under stress or magnetic field result

[5] Author to whom any correspondence should be addressed.

in a particular residual stress distribution. For a large and sensitive MI effect, it is essential that magnetic anisotropy is transverse with respect to the current and external field. Negative magnetostriction would be essential in this respect to establish a circumferential anisotropy. For example, in the case of Co-rich amorphous wires the negative magnetostriction coupled with the compressive stress arising from quenching results in a circumferential anisotropy and a circular domain structure. Such materials can be considered as one of the most suitable materials to observe the MI effects [17]. With respect to Fe-based materials, a distinct MI effect has not been achieved in any as-quenched Fe-based amorphous alloys except for the $Fe_{71}Zr_5B_{20}Nb_4$ ribbon [18], as the Fe-based material has a positive magnetostriction that results in a longitudinal magnetic structure in the case of tensile internal stress. Stress annealing treatment of amorphous alloys was proposed to change the stress-induced anisotropy by establishing frozen-in compression stress [19].

Recently, some nanocrystalline magnetic alloys consisting of bcc nanoscale crystalline phase have been obtained by crystallizing melt-spun amorphous samples [20–22]. Since the nanograins are magnetically coupled through the ferromagnetic amorphous matrix, the apparent magnetocrystalline anisotropy is averaged out and the materials exhibit rather good soft magnetic properties [23]. Fe–Zr–B nanocrystalline alloy, widely known as NANOPERM, is one of the most extensively studied nanostructured Fe-based materials. Following the first discovery of nanocrystalline Fe–Si–B based soft magnetic material by Yoshizawa *et al* [24], Fe–Zr–B based nanocrystalline alloys was developed by Suzuki *et al* in 1991 [25]. After that, Wu *et al* [26] found it possible to improve the magnetic properties of the $(Fe_{90}Zr_7B_3)_{1-x}(Fe_{84}Nb_7B_9)_x$ alloys by making a uniform nanocrystalline microstructure by adding Cu as a nucleation agent. Moreover, many reports [27–29] confirmed that the addition of TM = Zr, Nb, Mn and Hf atoms into Fe–TM–B–(Cu) alloys improved their soft magnetic properties. Simultaneously, the MI effect in FeZrB(Nb,Cu) nanostructured alloys was extensively investigated. For example, Lee *et al* [30] prepared nanocrystalline $Fe_{92-x-y}Zr_7B_xCu_1Al_y$ ($x = 2, 4, 6, 8$, $y = 0, 0.5, 1, 1.5$) ribbons and reported that the maximum MI ratio in the $Fe_{84}Zr_7B_8Cu_1$ alloy annealed at 550 °C was reached as much as 1100% at 4.6 MHz. In another case, the MI ratio of 480% was obtained at 1 MHz for the FeZrNbB ribbon annealed at 873 K with a tensile stress of 52 MPa [31]. According to the study of He *et al* [7], the maximum MI value of about 260% was achieved in the $Fe_{84}Zr_7B_8Cu_1$ ribbon annealed at 873 K for 20 min at frequency $f = 6.5$ MHz.

In this paper, our efforts have been devoted to investigating the MI effect in $Fe_{84.5}Zr_4B_{8.5}Nb_2Cu_1$ ribbons in the as-quenched state and annealed at different temperatures and analyzing the nanostructures that affect the magnetic properties and hence the MI behaviour of the alloy. According to our research results, the maximum MI ratio of $Fe_{84.5}Zr_4B_{8.5}Nb_2Cu_1$ is about 756% at 600 kHz accompanied by the field sensitivity of 108% Oe^{-1}, making the alloy more promising for technical applications in different kinds of high sensitivity micromagnetic sensors.

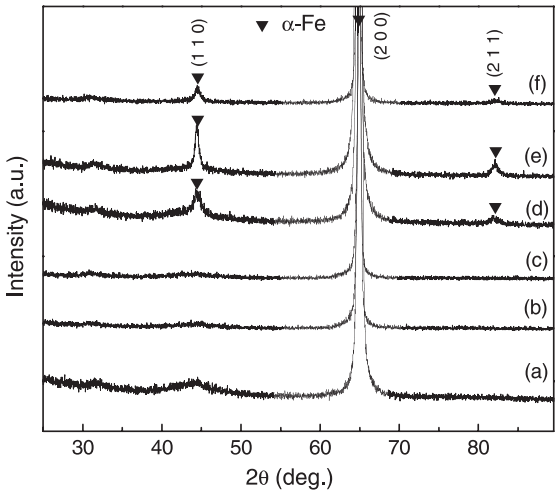

Figure 1. X-ray diffraction patterns of $Fe_{84.5}Zr_4B_{8.5}Nb_2Cu_1$ ribbons in the as-quenched state (a) and annealed at 245 °C (b), 385 °C (c), 495 °C (d), 575 °C (e) and 665 °C (f) for 20 min.

2. Experimental procedures

$Fe_{84.5}Zr_4B_{8.5}Nb_2Cu_1$ (FZBNC) ribbons about 1.2 mm in width and 50 μm in thickness were prepared by a rapid quenching technique in an argon atmosphere. The as-quenched state of the ribbons was examined by the x-ray diffraction technique, confirming that the FZBNC were not fully amorphous alloys. Afterwards, the as-quenched samples were annealed at 245 °C, 385 °C, 495 °C, 575 °C and 665 °C for 20 min, respectively, in a high vacuum condition to the order of 10^{-3} Pa, then cooled naturally at the room temperature. Magnetization measurements were carried out using a vibrating sample magnetometer (VSM). Electrical resistivity measurements were performed by the four-terminal method.

In order to measure the MI, the ribbons were connected in series with a resistor. The ac driving current passed through the sample and created a transverse ac magnetic field that magnetized the ribbon in the transverse direction, inducing a voltage between the ends of the sample. A four-probe technique was used to measure the induced voltage that is proportional to the magnitude of impedance (Z), as a function of the field (H) applied along the ribbon length (about 70 mm), i.e. parallel to the ac measuring current. The current amplitude was kept constant ($I = 10$ mA) and the frequency (f) was between 600 kHz and 2 MHz. The external field was generated by a pair of Helmholtz coils with the axis perpendicular to the Earth's magnetic field to allow the field variation from 0 to 60 Oe.

3. Results and discussion

3.1. Microstructural analyses

Figure 1(a)–(f) shows the x-ray diffraction patterns from the free surface of the as-quenched and annealed FZBNC ribbons. The bcc α-Fe phase is identified from each of the XRD patterns. For the FZBNC alloys in the as-quenched state and annealed at 245, 385 °C (see figure 1(a)–(c)), the peak of α-Fe represent (2 0 0) diffraction. For the samples annealed at 495 °C, 575 °C and 665 °C (see figure 1(d)–(f)), the three peaks of α-Fe (from

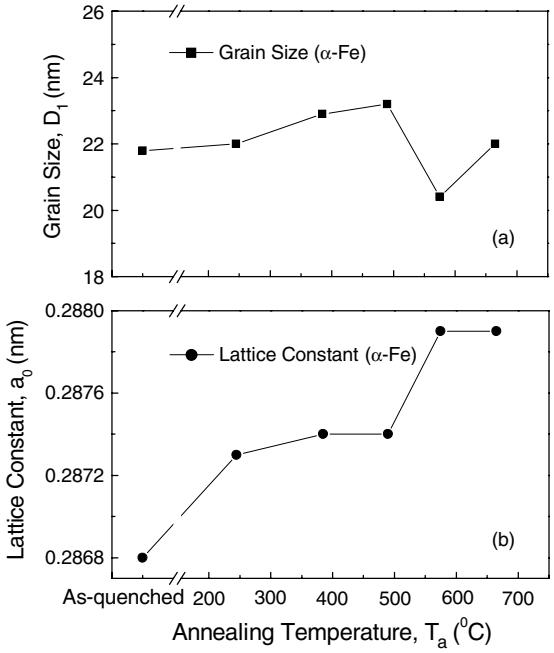

Figure 2. Annealing temperature (T_a) dependence of the grain size (α-Fe) (D_1) (*a*) and the lattice constant (α-Fe) (a_0) (*b*).

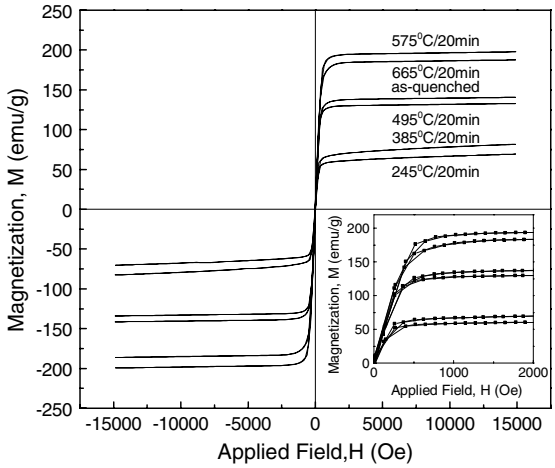

Figure 3. The longitudinal hysteresis loops of $Fe_{84.5}Zr_4B_{8.5}Nb_2Cu_1$ ribbons in the as-quenched state and annealed at various temperatures. The inset of the figure shows the open/full points of the hysteresis loops in the positive magnetic field.

left to right) represent (1 1 0), (2 0 0) and (2 1 1) diffraction, respectively. When the annealing temperature is higher than 495 °C, the residual amorphous FZBNC crystallizes to α-Fe, so the (1 1 0) and (2 1 1) diffraction peaks appear. Moreover, it can be found from figure 1 that the intensity of (2 0 0) diffraction of α-Fe is stronger than that expected from the randomly oriented polycrystal, suggesting that α-Fe crystals are strongly textured in the free surface of FZBNC ribbons [26].

In order to find out the microstructural changes of FZBNC alloy with isothermal heat treatment conditions, the mean grain size of the α-Fe phase (D_1) at different annealing temperatures (T_a) was estimated by using Scherrer's equation from the half width of the (2 0 0) diffraction peak, and the variation of D_1 with T_a is shown in figure 2(*a*). It can be seen clearly from figure 2(*a*) that D_1 is less than 22 nm in the as-quenched state, slightly increasing with the increment of T_a to about 23 nm, and abruptly diminishes to around 20 nm at 575 °C. When T_a is higher than 575 °C, D_1 starts to increase again. According to some previous studies [27, 32], a sudden decrease in the mean grain size with the increasing annealing temperature was also observed. In this experiment, as shown in the following context, the sample annealed at 575 °C exhibits the best soft magnetic properties, which is correlated with the smaller mean grain size. The lattice constant of the α-Fe (a_0) versus T_a curve is also plotted in figure 2(*b*). From figure 2(*b*) we can observe that a_0 goes up with increasing annealing temperature and is larger than the normal value (2.866 Å) at every stage. Besides, a_0 increases drastically after 495 °C and then keeps almost constant. The observed larger lattice parameter is due to Zr and B elements dissolving in the bcc phase [33]. After 575 °C, the unchangeableness of the lattice parameter is attributed to the saturation of elements dissolution.

3.2. Magnetic and electrical properties

As is known, the microstructures of nanocrystalline alloys as well as the chemical compositions of the constituent phases tend to affect the magnetic and electrical properties of materials. Fe–Zr–B amorphous alloys have been reported to exhibit excellent soft magnetic properties after being annealed under optimal conditions, when they reach a nanocrystalline (Nanoperm) microstructure characterized by a nanometric bcc-Fe phase surrounded by a residual amorphous matrix [34].

For the better understanding of the magnetic properties of FZBNC alloys, longitudinal hysteresis loops have been studied and plotted in figure 3. The inset of the figure shows the open/full points of the hysteresis loops in the positive magnetic field. Each of the hysteresis loops (as shown in figure 3) approaches the *y*-axis, indicating that the samples are easily magnetized in the longitudinal direction. In view of seeing the changes in the magnetic properties at different temperatures, the coercivity (H_c) as well as relative permeability (μ') and saturation magnetization (M_s) have been evaluated from the hysteresis loops. The T_a dependence of these parameters is shown in figures 4(*a*), (*b*) and (*c*), respectively. According to the results as shown in figure 4(*a*), H_c decreases tardily at first and then rapidly with increasing annealing temperature. The reduction of H_c at 245 °C is associated with the release of the residual stresses remaining in the sample during fabrication. After 495 °C, H_c changes slightly and reaches the smallest value at 575 °C, indicating that FZBNC alloys annealed at higher temperatures exhibit excellent soft magnetic properties. (The data of H_c in our experiments were obtained by using a VSM that is not as precise as the special instrument for coercivity measurement. Generally speaking, the data of the coercive force obtained from VSM are somewhat larger. However, the changing tendency of H_c with T_a is creditable.) Additionally, as shown in figure 4(*b*), the T_a dependence of the μ' curve indicates that the permeability of FZBNC decreases at first and then increases after 245 °C, approaching the largest value at 575 °C. When the annealing temperature continues to increase, μ' goes slightly down. The change in M_s with T_a plotted in figure 4(*c*) exhibits

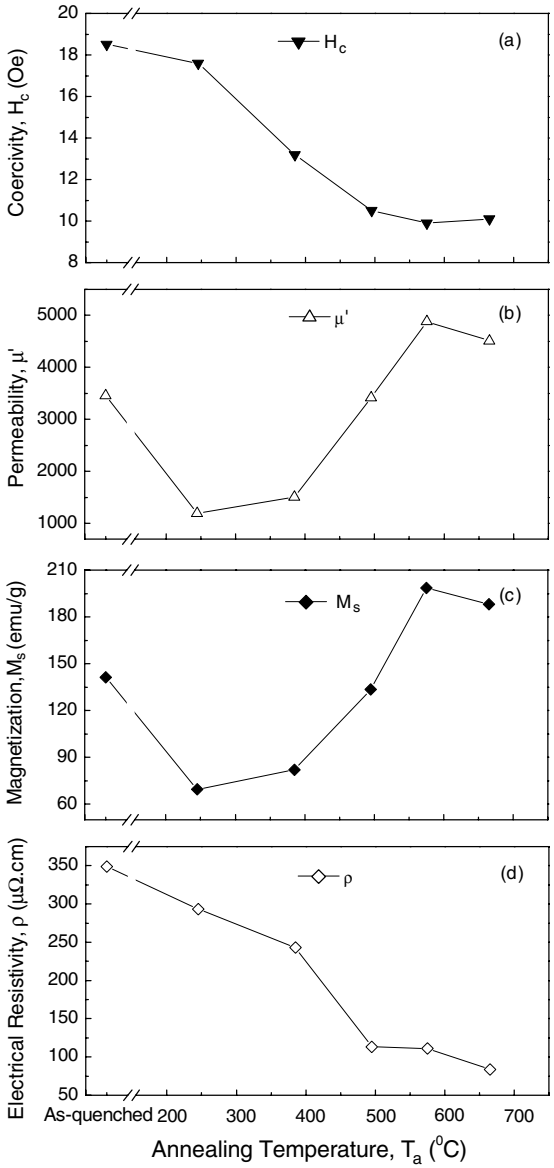

Figure 4. Annealing temperature (T_a) dependence of coercivity H_c (*a*), permeability μ' (*b*), saturation magnetization M_s (*c*) and electrical resistivity ρ (*d*).

almost the same changing tendency as that in figure 4(*b*). Both the above results further confirm that FZBNC alloys annealed at higher temperatures possess better soft magnetic properties. The origin of the excellent soft magnetic properties for the nanocrystalline alloys has been explained on the basis of the random anisotropy model [35], which states that the magnetocrystalline anisotropy is averaged out due to strong ferromagnetic exchange coupling between the ferromagnetic grains. During the process of crystallization, unavoidable changes take place in the residual amorphous phase. As the exchange coupling is conveyed only through the intergranular amorphous phase, any variation in the magnetic nature of the amorphous phase will consequently change the intergrain exchange coupling and then alter the magnetic properties of the samples. According to the studies of Bitoh *et al* [36], the soft magnetic properties of Fe–Nb–Zr–B–Cu are dominated by not only the grain size of the bcc phase but also the Curie temperature of the intergranular amorphous phase. If the Curie temperature of the residual amorphous phase is low, it cannot fully mediate the intergranular exchange coupling at room temperature due to the thermal fluctuation of the spins in the amorphous phase. The Curie temperature of the residual amorphous phase was evaluated from the inflection points of the B_s^3–T curves (B_s is high saturation magnetic flux density) [36]. It is difficult to determine the Curie temperature (amorphous) exactly because the change in B_s due to the ferromagnetic to paramagnetic phase transition of the residual amorphous phase is very small. However, it can be said that with increasing annealing temperature, the Curie temperature (amorphous) increases and the exchange coupling between the bcc grains is enhanced. On the other hand, in the higher annealing temperature range, the deterioration of the magnetic softness by the increase in the grain size probably becomes dominant.

Moreover, by adjusting the annealing conditions, λ_s can also be controlled. In conformity to the study of Suzuki *et al* [34], λ_s of Fe–Zr–B–Cu decreases from a large positive value to a negative one passing through zero with increasing annealing temperature, and the maximum permeability is obtained at the smallest magnitude of λ_s. The balanced magnetostriction is due to the opposite contribution to this parameter from the α-Fe nanocrystals and from the amorphous matrix. In our experiments, consequently, it is deduced that the small negative magnetostriction that is closely related to a significant MI effect may be obtained in the specimen annealed at 575 °C.

Besides, the electrical resistivity (ρ) of FZBNC alloys has been measured and the T_a dependence of ρ is plotted in figure 4(*d*). From figure 4(*d*) it is noted that the electrical resistivity of FZBNC shows a diminishable trend in the whole temperature range. When the temperature reaches 495 °C, ρ goes down suddenly to a great extent, which is correlated with the crystallization of residual amorphous FZBNC and the appearance of a large amount of the α-Fe phase. As is known the MI effect has a classical electromagnetical origin being related to the penetration depth δ, which is defined as (in CGS units) [37]

$$\delta = 5030\left(\frac{\rho}{\mu f}\right)^{1/2}, \qquad (1)$$

where ρ is the electrical resistivity, μ is the transverse magnetic permeability and f is the driving field frequency. In the case of alloys with longitudinal anisotropy, to achieve a large MI effect, the penetration depth should be very small in the absence of any applied field, which can be increased with the application of a dc magnetic field. The high value of frequency, large transverse magnetic permeability and low value resistivity give rise to a small penetration depth in the absence of any external magnetic field. According to some research results [38,39], the smaller the electrical resistivity of the sample, the larger the MI value obtained. But in systems with transverse anisotropy, the situation can be quite opposite when the penetration depth is large at zero field and it decreases greatly with the application of the field.

3.3. MI effect

The impedance Z of the FZBNC alloy, as a function of the external longitudinal dc field, was measured at 600 kHz,

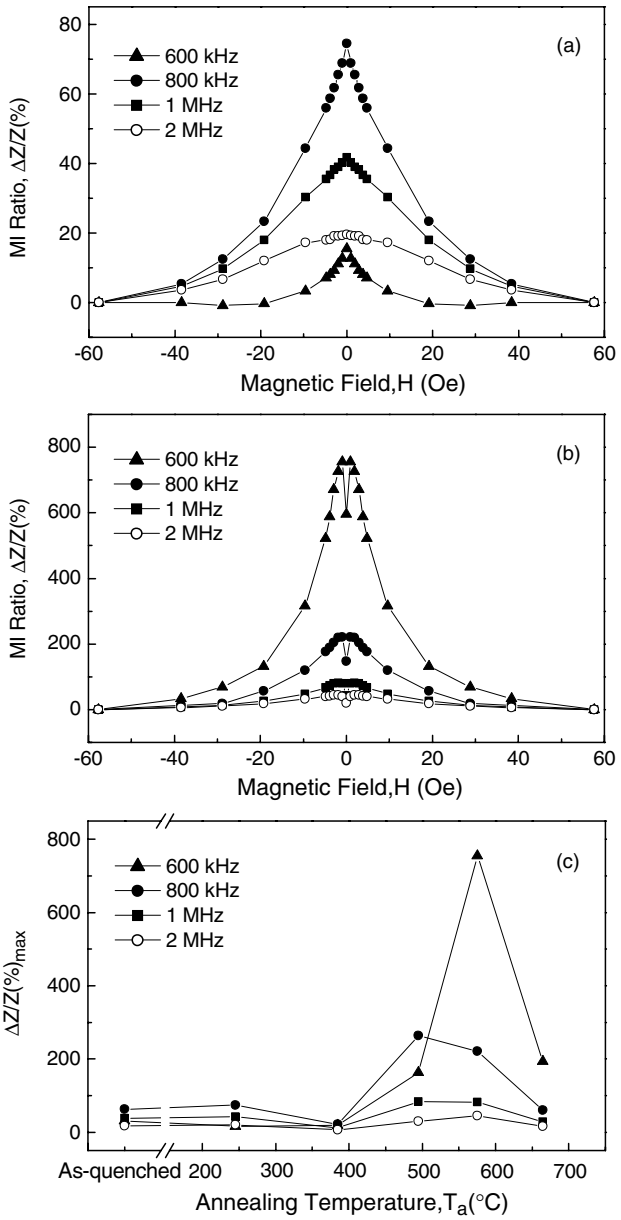

Figure 5. Field dependence of the MI ratio, defined as $\Delta Z/Z(\%) = [Z(H) - Z(H_{max})]/Z(H_{max})$, for $Fe_{84.5}Zr_4B_{8.5}Nb_2Cu_1$ alloys annealed at 245 °C (*a*) and 575 °C (*b*). Annealing temperature (T_a) dependence of the maximum MI ratio ($\Delta Z/Z(\%)_{max}$) (*c*).

800 kHz, 1 MHz and 2 MHz. The MI ratio $\Delta Z/Z(\%)$ denotes $[Z(H) - Z(H_{max})]/Z(H_{max})$, in which $Z(H_{max})$ is the impedance value under the maximum magnetic field of 57.6 Oe. Figure 5(*a*) shows the field dependence of the MI ratio for the FZBNC ribbon annealed at 245 °C at various frequencies. It is found that the MI ratio decreases monotonously with the applied magnetic field under the measuring frequencies. In general, there are two types of MI curves, which depend on the effective anisotropy in the sample [37,40,41]. For a single-peak behaviour, a longitudinal anisotropy with respect to the current and the applied current is essential. The ac magnetization precession occurs under the effect of a transverse ac magnetic field induced by the current. The value of the anisotropy influences only on the sensitivity. For a two-peaks curve, a transverse anisotropy with respect to the current and the field is essential. In the present work, the MI curves for the FZBNC ribbon annealed at 245 °C belong to the former case. In addition, as observed in figure 5(*a*), the MI effect is more obvious at 800 kHz than at other frequencies. The largest MI value observed in the sample is about 75%. The MI effect in FZBNC alloys in the as-quenched state and annealed at 385 °C also displays a similar changing tendency.

The field dependence of the MI ratio of the FZBNC ribbon annealed at 575 °C at various frequencies is plotted in figure 5(*b*). In contrast to the curves shown in figure 5(*a*), a two-peaks behaviour is observed for the sample annealed at 575 °C. Previous studies have established that the appearance of double peaks is due to transverse anisotropy. At zero applied field when the magnetization is in the transverse direction, the ac precession under the transverse ac magnetic field is not possible. Applying the dc field and rotating the magnetization away from the transverse direction stimulates the precession and larger ac permeability is established [15, 42]. When a small static magnetic field is applied along the length of the ribbon, the domain walls move along the length of the ribbon. This happens until the static field reaches the anisotropy field H_k. Further increase in the static field could inhibit the wall movement and impel the rotation of the domains as the effective transverse permeability decreases sharply leading to a strong MI effect. The two-peaks behaviour confirms the damping of domain wall motions and shows that tangential magnetization proceeds by the rotation of the domains [11]. From figure 5(*b*) it can be observed that the effective anisotropy field is about 1 Oe at the measuring frequency of 600 kHz and changes to a larger value with increasing frequency. Besides, the most evident MI effect is observed at the frequency of 600 kHz and the largest MI ratio observed is about 756%. With increasing frequency the MI response gradually diminishes. To clarify the field response of the MI effect at the measuring frequency, we calculate the field sensitivity of the MI effect for the sample, which is expressed as [43]

$$\xi = \frac{2[\Delta Z/Z(\%)_{max}]}{\Delta H}, \qquad (2)$$

where ΔH is the full width at half maximum of the MI response. The field sensitivity of the MI effect for the FZBNC at 600 kHz is 108% Oe^{-1}. These results are very promising for their application in the MI elements. The MI effect in FZBNC alloys annealed at 495 and 665 °C also displays a similar variation trend, except that the effective anisotropy field is larger in these two cases and the largest MI ratio for the specimen annealed at 495 °C occurs at the frequency of 800 kHz.

Moreover, the changes in the maximum MI ratio ($\Delta Z/Z(\%)_{max}$) with T_a at various frequencies are plotted in figure 5(*c*). It can be noted from figure 5(*c*) that the maximum MI ratios are comparatively small below the temperature of 385 °C. In the high temperature region, the MI effect is evidently larger than that observed in the low temperature region. In addition, the optimal frequency shifts towards the lower frequency value at 575 °C, which may be associated with the saturation of elements dissolution of the α-Fe phase. Furthermore, when T_a is higher than 575 °C, the MI effect goes down a great deal. The degradation of the MI effect in the

FZBNC annealed at 665 °C is attributed to the increase in the anisotropy and magnetostriction value, as well as the increment of the α-Fe grain size that is dominant in the deterioration of soft magnetic properties in the higher annealing temperature.

In summary, the analyses of the MI effect of the FZBNC alloys vividly demonstrate the crucial role of soft magnetic properties. The origin of the excellent soft magnetic properties displayed in the samples annealed at 575 °C lies in both the proper grain size of the α-Fe phase which is lower than the exchange correlation length and the Curie temperature of the intergranular amorphous phase. The greatest effect is also related to the change in the sign of the magnetostriction constant. λ_s of FZBNC may decrease from a large positive value to a negative one passing through zero with increasing annealing temperature and the small negative magnetostriction that is closely related to a significant MI effect may be obtained in the specimen annealed at 575 °C. Moreover, after suitable thermal treatment, a relatively small effective anisotropy develops in the FZBNC ribbons, which corresponds to a large MI effect. Owing to the complex magnetic response of the domain configuration or transversal magnetic permeability [22, 44–46], however, the emergence of effective anisotropy is difficult to explain in detail. Furthermore, the dimensions of FZBNC must be considered. The FZBNC ribbons have a thickness of 50 μm, thicker than the others previously reported, which is one of the important factors of the significant MI effect. The sample in the as-quenched state is partially crystallized, which is another important difference from other Fe-based ribbons.

4. Conclusions

The impact of nanocrystallization behaviour on the magnetic properties and the MI effect in the $Fe_{84.5}Zr_4B_{8.5}Nb_2Cu_1$ (FZBNC) ribbons has been studied. The bcc α-Fe phase is identified from the XRD patterns of all the investigated samples. Both the mean grain size of the nanocrystalline phases and the soft magnetic properties of FZBNC change with increasing annealing temperature. Concerning the MI effect, single-peak curves are observed for the samples in the as-quenched state and annealed at low temperatures. When the annealing temperature is higher than 495 °C, the MI effect exhibits a two-peaks behaviour and the maximum MI ratio is enhanced greatly. The significant MI effect in FZBNC annealed at 575 °C is attributed to the excellent soft magnetic properties, which are due to the proper grain size of the α-Fe phase and the Curie temperature of the intergranular amorphous phase. The greatest effect is also related to the change in the sign of the magnetostriction constant. Moreover, a relatively small effective anisotropy contributes to the significant MI behaviour also.

Acknowledgments

This work is supported by the National Natural Science Foundation (Grant No 50472003), Doctoral Foundation of Education Ministry of China (Grant No 20040183063) and the Creative Fund of Jilin University.

References

[1] Suzuki K, Kataoka N, Inoue A, Makino A and Masumoto T 1990 *Mater. Trans.* JIM **31** 743
[2] Makino A, Suzuki K, Inoue A and Masumoto T 1991 *Mater. Trans.* JIM **32** 551
[3] Makino A, Hatanai T, Inoue A and Masumoto T 1997 *Mater. Sci. Eng.* A **226–228** 594
[4] Panina L V, Mohri K, Bushida K and Noda M 1994 *J. Appl. Phys.* **76** 6198
[5] Beach R S and Berkowitz A E 1994 *J. Appl. Phys.* **76** 6209
[6] Knobel M, Sánchez M L, Velázquez J and Vázquez M 1995 *J. Phys.: Condens. Matter* **7** L115
[7] He J, Guo H Q, Shen B G, He K Y and Zhang H W 2001 *Mater. Sci. Eng.* A **304–306** 988
[8] Zhou Y, Yu J Q, Zhao X L and Cai B C 2001 *J. Appl. Phys.* **89** 1816
[9] Chen W P, Xiao S Q, Wang W J, Yuan H M and Liu Y H 2004 *J. Phys. D: Appl. Phys.* **37** 2780
[10] Li Y-F, Vázquez M and Chen D-X 2002 *J. Magn. Magn. Mater.* **249** 342
[11] Chiriac H, Óvári T A and Marinescu C S 1997 *IEEE Trans. Magn.* **33** 3352
[12] Zhou X Z, Tu G H, Kunkel H and Williams G 2006 *Sensors Actuators* A **125** 387
[13] Sinnecker J P, Sinnecker E H C P, Zhukov A, Garcia-Beneytez J M, Garcia Prieto J M and Vázquez M 1998 *J. Phys. IV* **8** Pr2–225
[14] Tejedor M, Hernando B, Sánchez M L, Prida V M and Vázquez M 1998 *J. Phys. D: Appl. Phys.* **31** 2431
[15] Makhnovskiy D P, Panina L V and Mapps D J 2001 *Phys. Rev.* B **63** 144424
[16] Morikawa T, Nishibe Y and Yamadera H 1997 *IEEE Trans. Magn.* **33** 4367
[17] Panina L V, Mohri K, Uchiyama T and Noda M 1995 *IEEE Trans. Magn.* **31** 1249
[18] Zhang K, Lv Z, Yao B and Wang D 2006 *J. Non-Cryst. Solids* **352** 78
[19] Zhukova V, Larin V S and Zhukov A 2003 *J. Appl. Phys.* **94** 1115
[20] He J, Guo H Q, Shen B G, He K Y and Kronmüller H 1999 *J. Appl. Phys.* **86** 3873
[21] Kamruzzaman Md, Rahman I Z and Rahman M A 2003 *J. Magn. Magn. Mater.* **262** 162
[22] Tejedor M, Hernando B, Sánchez M L, Prida V M, Garcia-Beneytez J M, Vázquez M and Herzer G 1998 *J. Magn. Magn. Mater.* **185** 61
[23] Herzer G 1989 *IEEE Trans. Magn.* **25** 3327
[24] Yoshizawa Y, Oguma S and Yamauchi K 1988 *J. Appl. Phys.* **64** 6044
[25] Suzuki K, Makino A, Kataoka N, Inoue A and Masumoto T 1991 *Mater. Trans. JIM* **32** 93
[26] Wu Y Q, Bitoh T, Hono K, Makino A and Inoue A 2001 *Acta Mater.* **49** 4069
[27] Müller M, Grahl H, Mattern N and Kühn U 1997 *Mater. Sci. Eng.* A **226–228** 565
[28] Kim K S, Yu S C, Moon Y M and Rao K V 1998 *J. Magn. Magn. Mater.* **177–181** 968
[29] Bitoh T, Nakazawa M, Makino A, Inoue A and Masumoto T 1999 *J. Appl. Phys.* **85** 5127
[30] Lee H, Lee K J, Kim Y K, Kim T K, Kim C O and Yu S C 2000 *J. Appl. Phys.* **87** 5269
[31] Gona M N, Yanase S, Hashi S and Okazaki Y 2003 *J. Magn. Magn. Mater.* **254–255** 466
[32] Hernando A and Kulik T 1994 *Phys. Rev.* B **49** 7064
[33] Yao B, Si L, Tan H, Zhang Y and Li Y 2003 *J. Non-Cryst. Solids* **332** 43
[34] Suzuki K, Makino A, Inoue A and Masumoto T 1991 *J. Appl. Phys.* **70** 6232
[35] Herzer G 1991 *Mater. Sci. Eng.* A **133** 1
[36] Bitoh T, Makino A, Hatanai T, Inoue A and Masumoto T 1997 *J. Appl. Phys.* **81** 4634

[37] Knobel M, Sánchez M L, Marín P, Gómez-Polo C, Vázquez M and Hernando A 1995 *IEEE Trans. Magn.* **31** 4009
[38] Knobel M, Sánchez M L, Gomez-Polo C, Marin P, Vázquez M and Hernando A 1996 *J. Appl. Phys.* **79** 1646
[39] Phan M H, Peng H X, Wisnom M R, Yu S C and Chau N 2004 *Phys. Status Solidi* a **201** 1558
[40] Chen C, Luan K Z, Liu Y H, Mei L M, Guo H Q, Shen B G and Zhao J G 1996 *Phys. Rev.* B **54** 6092
[41] Byon K S, Yu S C and Kim C G 2001 *J. Appl. Phys.* **89** 7218
[42] Makhnovskiy D P, Fry N, Panina L V and Mapps D J 2004 *J. Appl. Phys.* **96** 2150
[43] Hernando B, Sánchez M L, Prida V M, Tejedor M and Vázquez M 2001 *J. Appl. Phys.* **90** 4783
[44] Ueda Y, Ikeda S and Takakura W 1997 *J. Appl. Phys.* **81** 5787
[45] Tejedor M, Hernando B, Sánchez M L and Prida V M 1999 *J. Magn. Magn. Mater.* **203** 114
[46] Kurlyandskaya G V, García-Beneytez J M, Vázquez M, Sinnecker J P, Lukshina V A and Potapov A P 1998 *J. Appl. Phys.* **83** 6581